JACS
JOURNAL OF THE AMERICAN CHEMICAL SOCIETY
Communication
pubs.acs.org/JACS

Helical Conformation in the CA-SP1 Junction of the Immature HIV-1 Lattice Determined from Solid-State NMR of Virus-like Particles

Marvin J. Bayro,[†] Barbie K. Ganser-Pornillos,[‡] Kaneil K. Zadrozny,[‡] Mark Yeager,[‡,§,∥] and Robert Tycko*[,†]

[†]Laboratory of Chemical Physics, National Institute of Diabetes and Digestive and Kidney Diseases, National Institutes of Health, Bethesda, Maryland 20892-0520, United States

[‡]Department of Molecular Physiology and Biological Physics, University of Virginia School of Medicine, Seridan G. Snyder Translational Research Building, 480 Ray C. Hunt Drive, Charlottesville, Virginia 22908, United States

[§]Department of Medicine, Division of Cardiovascular Medicine, University of Virginia Health System, Charlottesville, Virginia 22908, United States

[∥]Center for Membrane and Cell Physiology, University of Virginia School of Medicine, Charlottesville, Virginia 22908, United States

Supporting Information

ABSTRACT: Maturation of HIV-1 requires disassembly of the Gag polyprotein lattice, which lines the viral membrane in the immature state, and subsequent assembly of the mature capsid protein lattice, which encloses viral RNA in the mature state. Metastability of the immature lattice has been proposed to depend on the existence of a structurally ordered, α-helical segment spanning the junction between capsid (CA) and spacer peptide 1 (SP1) subunits of Gag, a segment that is dynamically disordered in the mature capsid lattice. We report solid state nuclear magnetic resonance (ssNMR) measurements on the immature lattice in noncrystalline, spherical virus-like particles (VLPs) derived from Gag. The ssNMR data provide definitive evidence for this critical α-helical segment in the VLPs. Differences in ssNMR chemical shifts and signal intensities between immature and mature lattice assemblies also support a major rearrangement of intermolecular interactions in the maturation process, consistent with recent models from electron cryomicroscopy and X-ray crystallography.

In immature HIV-1, the inner leaflet of the viral membrane, is lined by a quasi-hexagonal two-dimensional lattice composed of ~5000 copies of the Gag polyprotein.[1] Maturation of HIV-1 involves an ordered sequence of proteolytic cleavages of Gag,[2] releasing separate matrix (MA), capsid (CA), nucleocapsid (NC), and p6 proteins, as well as "spacer peptides" that connect CA to NC (SP1) and NC to p6 (SP2). Cleavage at the CA-SP1 junction is thought to be the final step that permits disassembly of the immature Gag lattice and assembly of the CA lattice of the characteristic conical capsid,[3] which encloses viral RNA in association with NC within mature, infectious HIV-1.

Blockage of CA-SP1 cleavage by site-directed mutations[4] or by drugs known as maturation inhibitors,[5] such as bevirimat, prevents conversion of the immature Gag lattice to the mature CA lattice. Yet, in vitro, uncleaved CA-SP1 spontaneously self-assembles into the mature (not the immature) lattice structure, with the last 12 residues of CA and all 14 residues of SP1 forming a single, dynamically disordered C-terminal tail.[3,6] These observations support the idea that all or part of this 26-residue segment around the CA-SP1 junction (residues 220–245 of CA-SP1, or CA-SP1$_{220–245}$) is structurally ordered in the immature lattice, in a manner that locks the immature lattice in place as a metastable state until CA-SP1 cleavage occurs.[7] Biophysical studies suggest that a segment within CA-SP1$_{220–245}$ (equivalent to residues 352–377 of Gag) may adopt an α-helical conformation in the immature lattice.[8] Electron cryomicroscopy (cryoEM) images of immature HIV-1 show protein density consistent with a helical structure.[9] Very recently, a construct comprised of the C-terminal domain of CA and SP1 (CTD-SP1) has been crystallized into an immature-like lattice in which residues 225–238 form hexameric α-helical bundles.[10]

To investigate the CA-SP1$_{220–245}$ structure in the context of immature, spherical, virus-like particles (VLPs), we performed solid-state nuclear magnetic resonance (ssNMR) measurements on a 348-residue Gag construct (38.5 kDa) that contains residues 1–15 and 100–132 of MA and all of CA, SP1, and NC (ΔMA-CA-SP1-NC). CryoEM studies of these VLPs have shown that the ΔMA-CA-SP1-NC lattice recapitulates the Gag lattice in immature HIV-1.[1,7c,9c] All ssNMR measurements were performed at 14.1 T with 11.00 kHz magic-angle spinning, using a construct containing a Thr-to-Cys substitution at Gag residue 371 to increase the yield of VLPs (see Supporting Information). Transmission electron microscopy (TEM) images show that our ΔMA-CA-SP1-NC VLPs have uniform 100–120 nm diameters and are robust under ssNMR measurement conditions (Figure 1A,B).

As an initial test for structural order in the CA-SP1 junction, we prepared VLPs with ^{15}N,^{13}C-labeling of Val residues and ^{15}N-labeling of Leu residues, allowing the identification of ssNMR signals from the V230-L231 pair immediately before the CA-SP1 junction (Figure 1C). ssNMR signals from these residues are entirely absent from corresponding ssNMR spectra

Received: July 13, 2016
Published: September 5, 2016

DOI: 10.1021/jacs.6b07259
J. Am. Chem. Soc. 2016, 138, 12029–12032

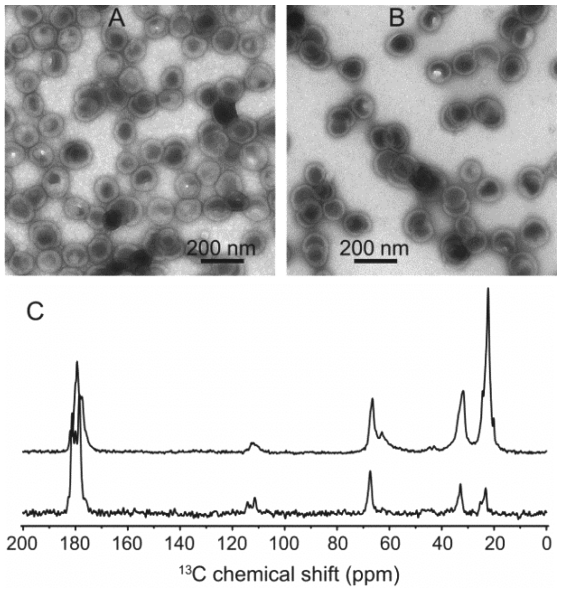

Figure 1. Sample assessment and detection of CA-SP1 junction residues. (A) Negatively stained TEM image of HIV-1 VLPs formed by spontaneous self-assembly of ΔMA-CA-SP1-NC. (B) Image after unpacking VLPs from the ssNMR rotor, following 96 h of data acquisition with magic-angle spinning at 11 kHz. (C) 1D ^{13}C ssNMR spectra of selectively Val/Leu-labeled VLPs, without (top) and with (bottom) ^{15}N filtering, showing the filtered V230 signal.

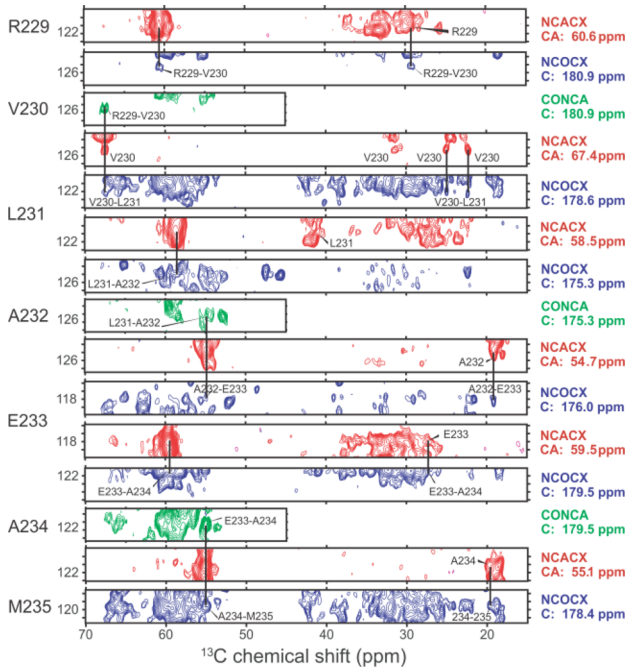

Figure 2. Sequential assignment of residues in the CA-SP1 junction from 3D NCACX (red), NCOCX (blue), and CONCA (green) ssNMR spectra of VLPs. 2D planes are shown with vertical axes labeled with the ^{15}N frequencies of the indicated residues. Vertical lines show sequential connections. Planes are taken at ^{13}C NMR frequencies indicated on the right.

of the mature lattice in CA assemblies, including tubular, spherical, and planar assemblies, due to dynamic disorder.[6c,11]

We then prepared uniformly ^{15}N,^{13}C-labeled VLPs and recorded two-dimensional (2D) and three-dimensional (3D) ssNMR spectra. Although these spectra are congested due to the high molecular weight of ΔMA-CA-SP1-NC (see Figures S1 and S2), chemical shifts for residues 216−241 (CA-SP1 numbering) were determined by standard methods of sequential resonance assignment (Figure 2, Table S1). Analysis of these chemical shifts with the TALOS-N program[12] yielded predictions of backbone ϕ and ψ torsion angles for residues 217−240, indicating an α-helical secondary structure from G225 to N240 (Figure 3A).

Results in Figure 3 represent direct experimental confirmation of structural order and α-helical conformation in the critical CA-SP1 junction within a noncrystalline, immature lattice formed by an HIV-1 Gag construct that includes full-length CA. Inclusion of full-length CA is important because the Gag lattice within immature HIV-1 is believed to be stabilized by intermolecular interactions involving both the N-terminal and the C-terminal domains of CA (NTD and CTD).[9b,c] Thus, our data support the notion of a helical bundle formed by CA-SP1 junction segments as a distinctive interaction stabilizing the immature lattice.[7,8] This helix appears to protect the scissile bond between CA and SP1 from protease cleavage, making this bond the final proteolytic site that triggers maturation. It seems likely that the helical CA-SP1 segment must unfold prior to proteolysis. This mechanism is analogous to the proposed transient unfolding that permits cleavage of the collagen triple helix by matrix metalloproteases.[13]

As shown in Figure 3B, analysis of chemical shifts by the MICS program[14] suggests a type II β-turn in residues 220−223 (GVGG sequence). This β-turn is also observed in the recent CTD-SP1 crystal structure, where it forms multiple intermolecular contacts and orients the junction helix into the stem

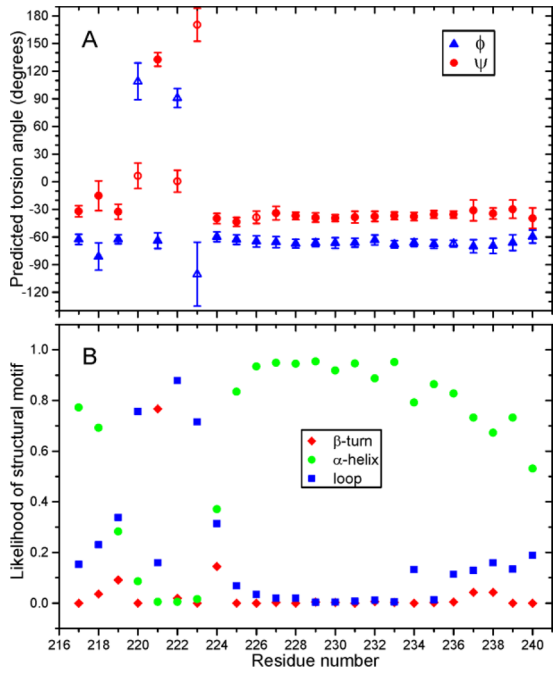

Figure 3. Secondary structure in the CA-SP1 junction within VLPs. (A) Backbone torsion angle predictions from chemical shift analysis based on ^{15}N and ^{13}C ssNMR signals of VLPs. Filled symbols are classified as strong predictions by TALOS-N. Residues 225−240 of CA-SP1 ($Gag_{357-372}$) adopt torsion angles indicative of an α-helical conformation. (B) Residue-specific likelihoods of α-helix, type II β-turn, and loop conformations from MICS. Values for β-turn are plotted on the second residue of a four-residue segment, suggesting a β-turn in residues 220−223.

DOI: 10.1021/jacs.6b07259
J. Am. Chem. Soc. 2016, 138, 12029−12032

region of the goblet-like CTD-SP1 hexamer.[10] ssNMR measurements of $^{15}N-^{15}N$ dipole–dipole couplings indicate good agreement of backbone conformations at G220 and V230 between VLPs and the CTD-SP1 crystal structure (Figure S3). In contrast, residues 220–223 are dynamically disordered in tubular CA assemblies,[6c,11a] unobserved in crystal structures of mature capsid constructs,[15] and disordered in structure bundles from solution NMR of CTD, CA, and full-length Gag.[16] However, backbone torsion angles predicted from chemical shifts of soluble, unassembled CA constructs (Figure S4) are similar to those obtained from our ssNMR data for VLPs. Therefore, it appears that residues 220–223 of CA have a propensity to form a β-turn in solution, and that the β-turn is only stabilized in the assembled immature lattice, concomitantly with formation of the CA-SP1 helix. Conversely, the inherent flexibility of this short segment may play a role in the unfolding of CA-SP1 helices prior to protease cleavage.

The immature Gag lattice is stabilized primarily by intermolecular interactions among CA subunits, with MA serving to tether the immature lattice to the viral membrane and NC serving to bind RNA. Although immature and mature assemblies are both triangular lattices of CA hexamers, cryoEM of immature HIV-1 indicates that the intermolecular interactions of both NTD and CTD are quite different in the two lattices (Figures 4A–C and S5).[9a,b] For CTD, this finding is borne out by the crystal structure of CTD-SP1.[10] To identify additional evidence for structural rearrangements involving both NTD and CTD, we obtained partial chemical shift assignments for these domains from the 3D ssNMR spectra of ΔMA-CA-SP1-NC VLPs and compared them with our previously reported ssNMR data for tubular CA assemblies, which contain the mature lattice.[11a] Assignments were facilitated by the flexibility of ΔMA and NC domains, which contribute few signals to the ssNMR spectra of VLPs, since the ssNMR measurement conditions favor immobilized segments. In cases where direct comparison of VLP spectra and CA tube spectra did not yield unambiguous assignments, due to large resonance shifts or spectral overlap, we used sequential correlations to verify the assignments.

Figure 4D shows the differences in chemical shifts between CA tubes and VLPs (Biological Magnetic Resonance Bank accession numbers 19575 and 26883). Many differences are observed, indicating many structural differences at the residue-specific level. Figure 4E depicts the secondary structure of CA, the intermolecular interfaces in mature CA and immature Gag lattices, and the locations where significant differences in chemical shifts or ssNMR signal amplitudes are observed. Differences in chemical shifts or signal amplitudes are observed in all interface segments, supporting the notion that mature and immature lattices are formed by entirely different interactions between CA domains. Importantly, these correlations between spectral changes and differences in intermolecular interface differences verify that our ΔMA-CA-SP1-NC VLPs have a different supramolecular architecture than mature CA assemblies.

Differences in signal amplitudes imply site-specific differences in dynamics or in structural homogeneity between the two types of assemblies. In the mature lattice, residues 1–13 form a partially ordered β-hairpin,[15b] with strong signals from residues 1–6 in ssNMR spectra of CA tubes.[11a] These signals are absent from ssNMR spectra of VLPs, as expected if the covalent linkage to ΔMA prevents β-hairpin formation at the N-terminal segment of CA. On the other hand, the C-terminal segment of

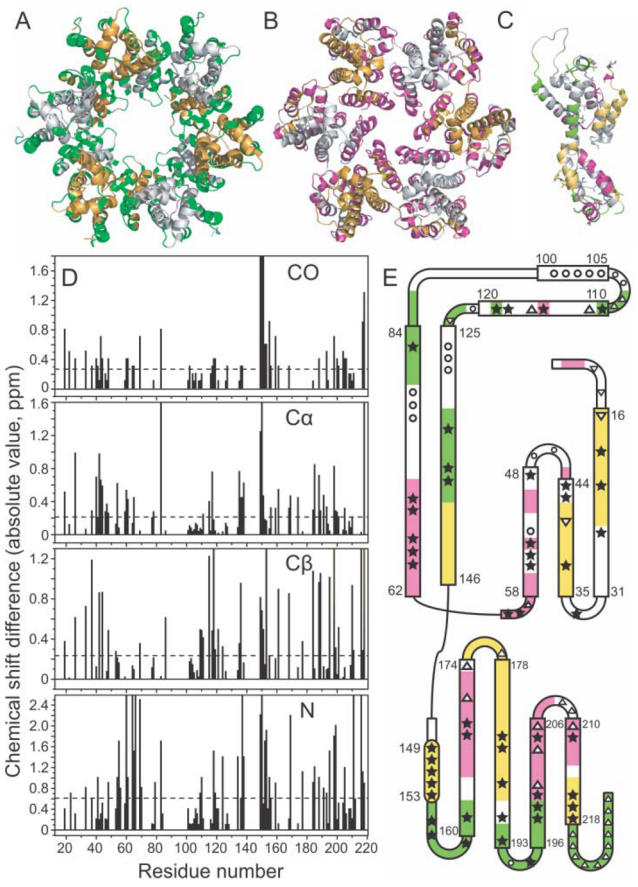

Figure 4. Differences in structure between immature and mature HIV-1 lattices. (A,B) CA hexamers in immature and mature lattices (PDB files 4USN and 4XFX, respectively), with residues involved in intermolecular interfaces colored green and pink, respectively. Other residues are colored gray and orange, alternately around each hexamer. (C) CA monomer, with immature and mature interface residues colored green and pink. Residues with interface contacts in both lattices are colored yellow, although these contacts usually involve different partners in the two lattices. (D) Absolute values of chemical shift differences between ΔMA-CA-SP1-NC VLPs and CA tubes for CO, C_α, C_β, and backbone N sites. (E) Schematic representation of sites in the CA sequence with chemical shift differences greater than $1.5\Delta_{RMS}$ (filled stars) or less than $0.5\Delta_{RMS}$ (open circles), or with significant changes in ssNMR signal amplitudes (open triangles). Green, pink, and yellow segments are defined as in panel C. White segments have no intermolecular contacts in either lattice.

CA, which is invisible in ssNMR spectra of CA tubes,[11a] becomes visible in VLPs, as discussed above.

Signal amplitude differences in other regions of the CA sequence can be understood by differences in supramolecular structure. For example, while helix 10 (residues 196–206) forms a trimeric interface in the mature CA lattice,[17] this trimeric interface is absent from the immature lattice (see Figure S5). A number of sites at the end of helix 10 and in the loop between helices 10 and 11 (residues 204–210) have increased signal amplitudes in ssNMR spectra of VLPs compared to spectra of CA tubes. Additionally, in the mature lattice of CA tubes, the loop between helices 8 and 9 (residues 160–174 and 178–193) of CTD makes intramolecular contacts with NTD, possibly with a distribution of conformations due to flexibility in the CTD-NTD linker.[18] According to cryoEM of immature HIV-1, intramolecular

DOI: 10.1021/jacs.6b07259
J. Am. Chem. Soc. 2016, 138, 12029–12032

NTD−CTD distances are larger in the immature lattice.[9b] Correspondingly, signal amplitudes from Ala174 and Ala177 are larger in ssNMR spectra of VLPs.

Examples of spectral comparisons between VLPs and CA tubes are shown in Figure S6, and locations of spectral changes are indicated on the structure of CA in Figure S7. In contrast to the spectral changes observed for residues that are involved in intermolecular interfaces, multiple contiguous residues with negligible changes in chemical shifts (less than $0.5\Delta_{RMS}$, open circles in Figure 4E) are found in segments that do not establish interfaces in either type of assembly.

In conclusion, ssNMR data for ΔMA-CA-SP1-NC VLPs indicate the existence of a 16-residue α-helical segment around the CA-SP1 junction in the Gag lattice of immature HIV-1, providing direct support for the idea that helical structure in this segment stabilizes the immature lattice and inhibits HIV-1 maturation by blocking protease access to the CA-SP1 cleavage site. These data also indicate the feasibility of future ssNMR studies to sharpen our understanding of aspects of the Gag lattice that remain uncertain, such as the detailed structure of key intermolecular interfaces,[19] and to identify the binding modes of maturation inhibitors.

■ ASSOCIATED CONTENT

Supporting Information

The Supporting Information is available free of charge on the ACS Publications website at DOI: 10.1021/jacs.6b07259.

Materials and Methods section; additional ssNMR data for VLPs and comparisons with ssNMR spectra of CA assemblies; additional analysis of structural differences between immature and mature lattices, including Table S1 and Figures S1−S7 (PDF)

■ AUTHOR INFORMATION

Corresponding Author

*robertty@mail.nih.gov

Notes

The authors declare no competing financial interest.

■ ACKNOWLEDGMENTS

This work was supported by the Intramural Research Program of the National Institute of Diabetes and Digestive and Kidney Diseases and by the Intramural AIDS Targeted Antiviral Program of the National Institutes of Health (R.T.). This work was also supported by NIH grants R01-GM066087 (M.Y. and B.K.G.-P.) and P50-GM082545 (M.Y.).

■ REFERENCES

(1) Briggs, J. A. G.; Riches, J. D.; Glass, B.; Bartonova, V.; Zanetti, G.; Kräusslich, H. G. *Proc. Natl. Acad. Sci. U. S. A.* **2009**, *106*, 11090.

(2) Lee, S.-K.; Potempa, M.; Swanstrom, R. *J. Biol. Chem.* **2012**, *287*, 40867.

(3) de Marco, A.; Müller, B.; Glass, B.; Riches, J. D.; Kräusslich, H.-G.; Briggs, J. A. G. *PLoS Pathog.* **2010**, *6*, e1001215.

(4) (a) Guo, X.; Roldan, A.; Hu, J.; Wainberg, M. A.; Liang, C. *J. Virol.* **2005**, *79*, 1803. (b) Keller, P. W.; Johnson, M. C.; Vogt, V. M. *J. Virol.* **2008**, *82*, 6788.

(5) Keller, P. W.; Adamson, C. S.; Heymann, J. B.; Freed, E. O.; Steven, A. C. *J. Virol.* **2011**, *85*, 1420.

(6) (a) Meng, X.; Zhao, G.; Yufenyuy, E.; Ke, D.; Ning, J.; DeLucia, M.; Ahn, J.; Gronenborn, A. M.; Aiken, C.; Zhang, P. *PLoS Pathog.* **2012**, *8*, e1002886. (b) Keller, P. W.; Huang, R. K.; England, M. R.; Waki, K.; Cheng, N.; Heymann, J. B.; Craven, R. C.; Freed, E. O.; Steven, A. C. *J. Virol.* **2013**, *87*, 13655. (c) Han, Y.; Hou, G.; Suiter, C. L.; Ahn, J.; Byeon, I.-J. L.; Lipton, A. S.; Burton, S.; Hung, I.; Gor'kov, P. L.; Gan, Z.; Brey, W.; Rice, D.; Gronenborn, A. M.; Polenova, T. *J. Am. Chem. Soc.* **2013**, *135*, 17793. (d) Worthylake, D. K.; Wang, H.; Yoo, S.; Sundquist, W. I.; Hill, C. P. *Acta Crystallogr., Sect. D: Biol. Crystallogr.* **1999**, *55*, 85.

(7) (a) Pettit, S. C.; Moody, M. D.; Wehbie, R. S.; Kaplan, A. H.; Nantermet, P. V.; Klein, C. A.; Swanstrom, R. *J. Virol.* **1994**, *68*, 8017. (b) Accola, M. A.; Hoglund, S.; Gottlinger, H. G. A. *J. Virol.* **1998**, *72*, 2072. (c) Gross, I.; Hohenberg, H.; Wilk, T.; Wiegers, K.; Grättinger, M.; Müller, B.; Fuller, S.; Kräusslich, H. G. *EMBO J.* **2000**, *19*, 103.

(8) (a) Newman, J. L.; Butcher, E. W.; Patel, D. T.; Mikhaylenko, Y.; Summers, M. F. *Protein Sci.* **2004**, *13*, 2101. (b) Morellet, N.; Druillennec, S.; Lenoir, C.; Bouaziz, S.; Roques, B. P. *Protein Sci.* **2005**, *14*, 375. (c) Datta, S. A. K.; Clark, P. K.; Fan, L. X.; Ma, B. Y.; Harvin, D. P.; Sowder, R. C.; Nussinov, R.; Wang, Y. X.; Rein, A. *J. Virol.* **2016**, *90*, 1773.

(9) (a) Bharat, T. A. M.; Castillo Menendez, L. R.; Hagen, W. J. H.; Lux, V.; Igonet, S.; Schorb, M.; Schur, F. K. M.; Kräusslich, H.-G.; Briggs, J. A. G. *Proc. Natl. Acad. Sci. U. S. A.* **2014**, *111*, 8233. (b) Schur, F. K. M.; Hagen, W. J. H.; Rumlova, M.; Ruml, T.; Muller, B.; Krausslich, H.-G.; Briggs, J. A. G. *Nature* **2015**, *517*, 505. (c) Schur, F. K. M.; Obr, M.; Hagen, W. J. H.; Wan, W.; Jakobi, A. J.; Kirkpatrick, J. M.; Sachse, C.; Krausslich, H. G.; Briggs, J. A. G. *Science* **2016**, *353*, 506.

(10) Wagner, J. M.; Zadrozny, K.; Chrustowicz, J.; Purdy, M. D.; Yeager, M.; Ganser-Pornillos, B. K.; Pornillos, O. *eLife* **2016**, *5*, e17063.

(11) (a) Bayro, M. J.; Chen, B.; Yau, W.-M.; Tycko, R. *J. Mol. Biol.* **2014**, *426*, 1109. (b) Lu, J.-X.; Bayro, M. J.; Tycko, R. *J. Biol. Chem.* **2016**, *291*, 13098.

(12) Shen, Y.; Bax, A. *J. Biomol. NMR* **2013**, *56*, 227.

(13) Lu, K. G.; Stultz, C. M. *J. Mol. Biol.* **2013**, *425*, 1815.

(14) Shen, Y.; Bax, A. *J. Biomol. NMR* **2012**, *52*, 211.

(15) (a) Pornillos, O.; Ganser-Pornillos, B. K.; Kelly, B. N.; Hua, Y.; Whitby, F. G.; Stout, C. D.; Sundquist, W. I.; Hill, C. P.; Yeager, M. *Cell* **2009**, *137*, 1282. (b) Gres, A. T.; Kirby, K. A.; KewalRamani, V. N.; Tanner, J. J.; Pornillos, O.; Sarafianos, S. G. *Science* **2015**, *349*, 99.

(16) (a) Byeon, I.-J. L.; Meng, X.; Jung, J.; Zhao, G.; Yang, R.; Ahn, J.; Shi, J.; Concel, J.; Aiken, C.; Zhang, P.; Gronenborn, A. M. *Cell* **2009**, *139*, 780. (b) Shin, R.; Tzou, Y.-M.; Krishna, N. R. *Biochemistry* **2011**, *50*, 9457. (c) Deshmukh, L.; Ghirlando, R.; Clore, G. M. *Proc. Natl. Acad. Sci. U. S. A.* **2015**, *112*, 3374. (d) Deshmukh, L.; Schwieters, C. D.; Grishaev, A.; Ghirlando, R.; Baber, J. L.; Clore, G. M. *J. Am. Chem. Soc.* **2013**, *135*, 16133.

(17) Zhao, G.; Perilla, J. R.; Yufenyuy, E. L.; Meng, X.; Chen, B.; Ning, J.; Ahn, J.; Gronenborn, A. M.; Schulten, K.; Aiken, C.; Zhang, P. *Nature* **2013**, *497*, 643.

(18) (a) Pornillos, O.; Ganser-Pornillos, B. K.; Yeager, M. *Nature* **2011**, *469*, 424. (b) Byeon, I.-J. L.; Hou, G.; Han, Y.; Suiter, C. L.; Ahn, J.; Jung, J.; Byeon, C.-H.; Gronenborn, A. M.; Polenova, T. *J. Am. Chem. Soc.* **2012**, *134*, 6455.

(19) Bayro, M. J.; Tycko, R. *J. Am. Chem. Soc.* **2016**, *138*, 8538.

■ NOTE ADDED IN PROOF

Soon after initial submission of this paper, Schur et al. reported a cryoEM-based atomic model for similar VLPs, showing α-helix formation by CA-SP1 residues 225−239.[9c]

DOI: 10.1021/jacs.6b07259
J. Am. Chem. Soc. 2016, 138, 12029−12032